# Poster Contributions

https://doi.org/10.1017/S1743921318005227 Published online by Cambridge University Press

*Dwarf Galaxies: From the Deep Universe to the Present*
*Proceedings IAU Symposium No. 344, 2019*
*K. B. W. McQuinn & S. Stierwalt, eds.*

doi:10.1017/S1743921318005227

# Enrichment of Heavy Elements in Chemo-Dynamical Simulations of Dwarf Galaxies

**Yutaka Hirai[1], Takayuki R. Saitoh[2], Shinya Wanajo[3,4], and Michiko S. Fujii[5]**

[1]RIKEN Center for Computational Science,
7-1-26 Minatojima-minami-machi, Chuo-ku, Kobe, Hyogo 650-0047, Japan
email: yutaka.hirai@riken.jp

[2]Earth-Life Science Institute, Tokyo Institute of Technology, 2-12-1 Ookayama, Meguro-ku, Tokyo 152-8551, Japan

[3]Department of Engineering and Applied Sciences, Faculty of Science and Technology, Sophia University, 7-1 Kioicho, Chiyoda-ku, Tokyo 102-8554, Japan

[4]RIKEN iTHEMS Research Group, 2-1 Hirosawa, Wako, Saitama 351-0198, Japan

[5]Department of Astronomy, Graduate School of Science, The University of Tokyo, 7-3-1 Hongo, Bunkyo-ku, Tokyo 113-0033, Japan

**Abstract.** Abundances of heavy elements in dwarf galaxies reflect their early evolutionary histories. Recent astronomical observations have shown that there are star-to-star scatters in the abundances of $r$-process elements and the decreasing trend of Zn toward higher metallicity in extremely metal-poor stars. However, the enrichment of heavy elements is not well understood. Here we performed a series of high-resolution $N$-body/smoothed particle hydrodynamics simulations of dwarf galaxies. We find that neutron star mergers can explain ratios of $r$-process elements to iron in dwarf galaxies due to their suppressed star formation rates. We also find that stars with [Zn/Fe] $\gtrsim 0.5$ reflect the ejecta from electron-capture supernovae. Inhomogeneity of the metals in the interstellar medium causes the scatters of heavy elements. We estimate that the timescale of metal mixing is $\lesssim 40$ Myr using heavy element abundances in metal-poor stars.

**Keywords.** diffusion, galaxies: abundances, galaxies: dwarf, galaxies: evolution, hydrodynamics, ISM: abundances, methods: numerical, nucleosynthesis, stars: abundances, Local Group

## 1. Introduction

Understanding the enrichment of heavy elements in galaxies can lead to clarifying the evolutionary histories of galaxies. Stellar abundances of heavy elements reflect the astrophysical sites of elements and evolutionary histories of galaxies. Dwarf galaxies are ideal sites to study the enrichment of heavy elements. They contain many metal-poor stars which have different heavy element abundances, which point to the early evolutionary histories of galaxies.

It is possible to determine the abundances of heavy elements of each star in the Local Group dwarf galaxies. Elements which are synthesized by the rapid neutron-capture process (hereafter we call $r$-process elements) show characteristic abundances in the Local Group. Ji *et al.* (2016) and Roederer *et al.* (2016) reported that there are enhanced abundances of $r$-process elements in the Reticulum II ultra-faint dwarf galaxy (Ret II). On the other hand, in the classical dwarf spheroidal galaxies (dSphs), there are no $r$-process enhanced stars (e.g., Frebel & Norris 2015).

Abundances of Zn also show characteristic features in the Local Group galaxies. At [Fe/H] $\lesssim -2$, there is a decreasing trend toward higher metallicity in the ratios of [Zn/Fe] (e.g., Saito *et al.* 2009). Skúladóttir *et al.* (2017) showed that there are scatters in [Zn/Fe] ratios at [Fe/H] $\gtrsim -1.8$ in the Sculptor dSphs.

Although there are many observations of stellar abundances in dwarf galaxies, the enrichment of heavy elements in dwarf galaxies is not well clarified. The most promising sites of $r$-process elements are neutron star mergers (NSMs, e.g., Wanajo *et al.* 2014). Ishimaru *et al.* (2015) show that $r$-process elements increase at lower metallicity when they assume that smaller galaxies have lower star formation efficiencies. For Zn in dSphs, there are no studies so far in the context of chemical evolution in dwarf galaxies except for Hirai *et al.* (2018). It is necessary to perform a series of self-consistent chemo-dynamical simulations of dwarf galaxies to fully understand the enrichment of heavy elements. In this proceedings, we aim to report recent progress of our simulations regarding the enrichment of heavy elements.

## 2. Method

Here we briefly describe the adopted method in this study. We performed a series of $N$-body/smoothed particle hydrodynamics simulations with ASURA (Saitoh *et al.* 2008; 2009). The code adopts metallicity-dependent cooling/heating functions, star formation, and supernova feedback models (see Hirai *et al.* 2015 for datails). We treat star particles as a simple stellar population with the Kroupa *et al.* (2001) initial mass function from 0.1 to 100 $M_\odot$. We adopt the nucleosynthetic yields of core-collapse supernovae, hypernovae (HNe, Nomoto *et al.* 2013), electron-capture supernovae (ECSNe, Wanajo *et al.* 2018), NSMs (Wanajo *et al.* 2014), and type Ia supernovae (SNe Ia, Seitenzahl *et al.* 2013). These yields are compiled by chemical evolution library (CELib, Saitoh 2017). We assume that 5 % of stars with $\gtrsim 20$ $M_\odot$ explode as HNe. Mass ranges of ECSNe are taken from stellar evolution calculations of Doherty *et al.* (2015). For NSMs and SNe Ia, we assume that power-law delay time distributions with the index of $-1$ and the minimum delay time of 10 and 100 Myr, respectively. The rate of NSMs is assumed to be consistent with the estimated rate by the gravitational wave observations (Abbott *et al.* 2017). For metal mixing, we adopt a shear-based metal mixing model (Shen *et al.* 2010; Saitoh 2017; Hirai & Saitoh 2017).

Here we compute an isolated dwarf galaxy model. We assume the pseudo-isothermal profile as the initial dark matter and gas density profiles (e.g., Revaz & Jablonka 2012). The total mass of the halo is $7\times10^8$ $M_\odot$. We set the total number of particles as $2^{18}$ with a gravitational softening length of 7 pc.

## 3. Results and Discussion

We confirm that our model has similar chemical evolution with the Sculptor dSph. Figure 1 (a) shows metallicity distribution functions computed in this model. The final median metallicity and stellar mass in this model are $\langle$[Fe/H]$\rangle = -1.3$ and $M_* = 3.7 \times 10^6$ $M_\odot$, respectively. These results are consistent with those of the Sculptor dSph ($\langle$[Fe/H]$\rangle = -1.7$ and $M_* = 3.9 \times 10^6$ $M_\odot$).

We compute the enrichment of Zn and $r$-process elements in this model. Figure 1 (b) depicts [Zn/Fe] as a function of [Fe/H]. At [Fe/H] $\lesssim -3$, there are stars with [Zn/Fe] ratios of $\gtrsim 0.5$ in this model. These stars are also seen in the observations. We find that these stars are formed from the ejecta from ECSNe. Stars which have [Zn/Fe] $\simeq 0.2$ at [Fe/H] $\lesssim -3$ are formed from the ejecta from HNe. Hirai *et al.* (2018) suggest that mass ranges of ECSNe affect the ratios of [Zn/Fe] at low metallicity. The decreasing trend toward higher metallicity seen at [Fe/H] $\gtrsim -2.5$ is due to the contribution of SNe Ia. We cannot see any significant scatters of [Zn/Fe] at [Fe/H] $\gtrsim -1.8$, which are implied in the

https://doi.org/10.1017/S1743921318005227 Published online by Cambridge University Press

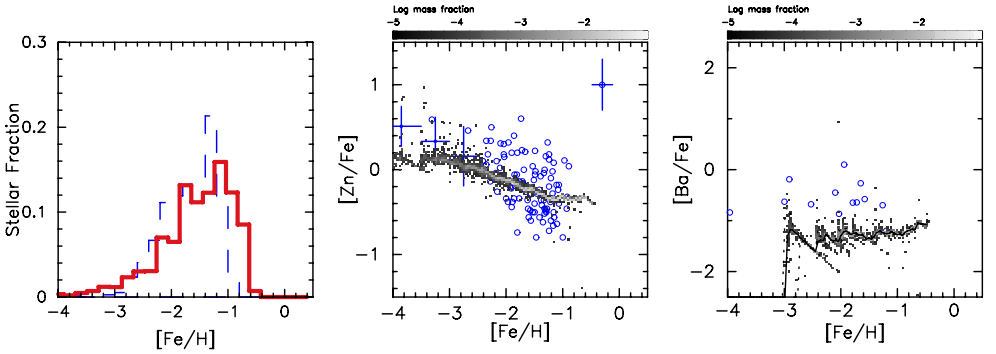


**Figure 1.** (a): Metallicity distribution functions of our model at 13.8 Gyr from the start of the simulation (red-solid histogram) and the Sculptor dSph (blue-dashed histogram; Kirby *et al.* 2009; 2010; Kirby & Cohen 2012). (b): [Zn/Fe] as a function of [Fe/H]. Grey scales show stellar mass fraction in each grid predicted by our model. Blue plots with error bars at [Fe/H] $< -2.5$ show observed data binned by Saito *et al.* (2009). Blue circles represent observed data of the Sculptor dSph (Shetrone *et al.* 2003; Geisler *et al.* 2005; Simon *et al.* 2015; Skúladóttir *et al.* 2017). Typical error bars are shown in the top right corner of the figure. (c): Same as (b) but for [Ba/Fe] as a function of [Fe/H]. Blue plots show observed data of the Sculptor dSph ((Shetrone *et al.* 2003; Geisler *et al.* 2005). All data are complied using SAGA database (Suda *et al.* 2008; 2017). Colour version is available online.

observations of Skúladóttir *et al.* (2017). This result suggests that the scatters seen in the Sculptor dSph come from observational errors or unknown sites of Zn synthesis such as zero-metallicity pair-instability supernovae (e.g., Heger & Woosley 2002).

Figure 1 (c) represents [Ba/Fe] as a function of [Fe/H]. We regard Ba as a representative of $r$-process elements because the pure $r$-process element, Eu is difficult to detect in the observation. Although most of Ba are synthesized by the $s$-process at high metallicity, we can regard Ba as $r$-process elements at [Fe/H] $\lesssim -2.5$ due to long lifetimes of low or intermediate mass stars which contribute to the $s$-process. As shown in this figure, NSMs can begin to occur at [Fe/H] $\sim -3$. This result is due to the suppressed star formation in dSphs (Hirai *et al.* 2015). When we fix the halo mass, NSMs begin to contribute at higher metallicity in galaxies with higher star formation rates (Hirai *et al.* 2017).

Abundances of heavy elements in metal-poor stars can be used as a tracer of metal mixing in galaxies. In classical dSphs, $r$-process enhanced stars ([Ba/Fe] $> 1$) has not been found. This result reflects the efficiency of metal mixing in galaxies. The results suggest that the scaling factor for metal mixing should be less than 0.01 to reproduce the observed lower ratios of $r$-process elements to iron in dSphs. Hirai & Saitoh (2017) show that the timescale of metal mixing corresponding to this efficiency is $\approx 40$ Myr. Enhanced $r$-process abundances seen in Ret II is due to a smaller initial gas mass of ultra-faint dwarf galaxies than that of classical dSphs (Ojima *et al.* 2018). Our results suggest that increasing the number of observations of $r$-process elements in dwarf galaxies can constrain the efficiency of metal mixing more precisely.

## Acknowledgements

This work was supported by JSPS KAKENHI Grant Numbers 18H05876, 26707007, 26400237, 26800108, MEXT SPIRE and JICFuS. YH conducts this study under the Special Postdoctoral Researcher Program, RIKEN. Numerical computations and analysis were in part carried out on Cray XC30, XC50, computers at CfCA, NAOJ and Cray XC40 at YITP in Kyoto University. This research has made use of NASA's Astrophysics Data System.

## References

Abbott, B. P. *et al.* 2017, *Phys. Rev. Lett.*, 119, 161101
Doherty, C. L., Gil-Pons, P., Siess, L., Lattanzio, J. C., & Lau, H. H. B. 2015, *MNRAS*, 446, 2599
Frebel, A., & Norris, J. E. 2015, *ARAA*, 53, 631
Geisler, D., Smith, V. V., Wallerstein, G., Gonzalez, G., & Charbonnel, C. 2005, *AJ*, 129, 1428
Ji A. P., Frebel A., Chiti A., & Simon J. D. 2016, *Nature*, 531, 610
Heger A., & Woosley S. E. 2002, *ApJ*, 567, 532
Hirai, Y., Ishimaru, Y., Saitoh, T. R., Fujii, M. S., Hidaka, J., & Kajino, T. 2015, *ApJ*, 814, 41
Hirai, Y., Ishimaru, Y., Saitoh, T. R., Fujii, M. S., Hidaka, J., & Kajino, T. 2017, *MNRAS*, 466, 2474
Hirai, Y., & Saitoh, T. R. 2017, *ApJ* (Letters), 838, L23
Hirai, Y., Saitoh, T. R., Ishimaru, Y., & Wanajo, S. 2018, *ApJ*, 855, 63
Ishimaru, Y., Wanajo, S., & Prantzos, N. 2015, *ApJ* (Letters), 804, L35
Kirby, E. N., & Cohen, J. G. 2012, *AJ*, 144, 168
Kirby, E. N., Guhathakurta, P., Bolte, M., Sneden, C., & Geha, M. C. 2009, *ApJ*, 705, 328
Kirby, E. N., Guhathakurta, P., Simon, J. D., Geha, M. C., Rockosi, C. M., Sneden, C., Cohen, J. G., Sohn, S. T., Majewski, S. R., & Siegel, M. 2010, *ApJS*, 191, 352
Kroupa, P. 2001, *MNRAS*, 322, 231
Nomoto, K., Kobayashi, C., & Tominaga, N. 2013, *ARAA*, 51, 457
Ojima, T., Ishimaru, Y., Wanajo, S., Prantzos, N., & François, P. 2018, *ApJ* in press, arXiv:1808.03390
Revaz, Y., & Jablonka, P. 2012, *A&A*, 538, A82
Roederer, I. U., Mateo, M., Bailey, J. I., Song, Y., Bell, E. F., Crane, J. D., Loebman, S., Nidever, D. L., Olszewski, E. W., Shectman, S. A., Thompson, I. B., Valluri, M., & Walker, M. G 2016, *AJ*, 151, 82
Saito, Y.-J., Takada-Hidai, M., Honda, S., & Takeda, Y. 2009, *PASJ*, 61, 549
Saitoh, T. R. 2017, *AJ*, 153, 85
Saitoh, T. R., Daisaka, H., Kokubo, E., Makino, J., Okamoto, T., Tomisaka, K., Wada, K., & Yoshida, N. 2008, *PASJ*, 60, 667
Saitoh, T. R., Daisaka, H., Kokubo, E., Makino, J., Okamoto, T., Tomisaka, K., Wada, K., & Yoshida, N 2009, *PASJ*, 61, 481
Seitenzahl, I. R., Ciaraldi-Schoolmann, F., Röpke, F. K., Fink, M., Hillebrandt, W., Kromer, M., Pakmor, R., Ruiter, A. J., Sim, S. A., & Taubenberger, S. 2013, *MNRAS*, 429, 1156
Shen, S., Wadsley, J., & Stinson, G. 2010, *MNRAS*, 407, 1581
Shetrone, M., Venn, K. A., Tolstoy, E., Primas, F., Hill, V., & Kaufer, A. 2003, *AJ*, 125, 684
Simon, J. D., Jacobson, H. R., Frebel, A., Thompson, I. B., Adams, J. J., & Shectman, S. A. 2015, *ApJ*, 802, 93
Skúladóttir, Á., Tolstoy, E., Salvadori, S., Hill, V., & Pettini, M. 2017, *A&A*, 606, A71
Suda, T., Hidaka, J., Aoki, W., Katsuta, Y., Yamada, S., Fujimoto, M. Y., Ohtani, Y., Masuyama, M., Noda, K., & Wada, K. 2017, *PASJ*, 69, 76
Suda, T., Katsuta, Y., Yamada, S., Suwa, T., Ishizuka, C., Komiya, Y., Sorai, K., Aikawa, M., & Fujimoto, M. Y. 2008, *PASJ*, 60, 1159
Wanajo, S., Müller, B., Janka, H.-T., & Heger, A. 2018, *ApJ*, 852, 40
Wanajo, S., Sekiguchi, Y., Nishimura, N., Kiuchi, K., Kyutoku, K., & Shibata, M. 2014, *ApJ* (Letters), 789, L39